El-Khatib *et al.*
Acta Neuropathologica Communications (2024) 12:190
https://doi.org/10.1186/s40478-024-01906-9

Acta Neuropathologica Communications

RESEARCH

Open Access

BDNF augmentation reverses cranial radiation therapy-induced cognitive decline and neurodegenerative consequences

Sanad M. El-Khatib[1], Arya R. Vagadia[1], Anh C. D. Le[1], Janet E. Baulch[2], Ding Quan Ng[4], Mingyu Du[3], Kevin G. Johnston[1,3], Zhiqun Tan[1,3], Xiangmin Xu[1,3], Alexandre Chan[4,5*] and Munjal M. Acharya[1,2*]

Abstract

Cranial radiation therapy (RT) for brain cancers is often associated with the development of radiation-induced cognitive dysfunction (RICD). RICD significantly impacts the quality of life for cancer survivors, highlighting an unmet medical need. Previous human studies revealed a marked reduction in plasma brain-derived neurotrophic factor (BDNF) post-chronic chemotherapy, linking this decline to a substantial cognitive dysfunction among cancer survivors. Moreover, riluzole (RZ)-mediated increased BDNF in vivo in the chemotherapy-exposed mice reversed cognitive decline. RZ is an FDA-approved medication for ALS known to increase BDNF in vivo. In an effort to mitigate the detrimental effects of RT-induced BDNF decline in RICD, we tested the efficacy of RZ in a cranially irradiated (9 Gy) adult mouse model. Notably, RT-exposed mice exhibited significantly reduced hippocampal BDNF, accompanied by increased neuroinflammation, loss of neuronal plasticity-related immediate early gene product, cFos, and synaptic density. Spatial transcriptomic profiling comparing the RT + Vehicle with the RT + RZ group showed gene expression signatures of neuroprotection of hippocampal excitatory neurons post-RZ. RT-exposed mice performed poorly on learning and memory, and memory consolidation tasks. However, irradiated mice receiving RZ (13 mg/kg, drinking water) for 6–7 weeks showed a significant improvement in cognitive function compared to RT-exposed mice receiving vehicle. Dual-immunofluorescence staining, spatial transcriptomics, and biochemical assessment of RZ-treated irradiated brains demonstrated preservation of synaptic integrity and mature neuronal plasticity but not neurogenesis and reduced neuroinflammation concurrent with elevated BDNF levels and transcripts compared to vehicle-treated irradiated brains. In summary, oral administration of RZ represents a viable and translationally feasible neuroprotective approach against RICD.

Keywords BDNF, Cranial radiation therapy, Cognitive function, Riluzole, Neuronal plasticity, Neuroinflammation

*Correspondence:
Alexandre Chan
a.chan@uci.edu
Munjal M. Acharya
macharya@uci.edu
Full list of author information is available at the end of the article

Introduction

With the growing annual incidence of cancer diagnoses, an increasing number of patients are undergoing conventional cancer treatment modalities including radiation therapy (RT). Whole and partial brain RT is a primary treatment modality for most brain cancers to improve the overall survival, palliation, or to control for the metastatic progression. In the United States, approximately 100,000 brain cancer patients receive RT every year, and about 50–90% of survivors display cognitive dysfunction [17, 56]. While RT has demonstrated efficacy as a therapeutic intervention, its unintended consequences, including memory loss, impaired concentration, cognitive processing difficulties, slow response speed, and compromised executive functioning, persist among patients post-RT [26, 39, 52]. Clinical reports indicate that these long-term side effects result from enduring structural changes in the brain post-RT [39]. The presence of prolonged and debilitating consequences of RT in the medical landscape underscores the need for developing translationally feasible therapeutic approaches to mitigate cognitive decline and improve patients' overall quality of life [43].

Clinical investigations have revealed a noteworthy correlation between the levels of brain-derived neurotrophic factor (BDNF) and cognitive outcomes in cancer patients exposed to systemic chemotherapy [44, 45]. A breadth of literature has established the link between lower BDNF levels in individuals diagnosed with neurodegenerative disorders such as Huntington's disease (HD), Alzheimer's disease (AD), and multiple sclerosis (MS) [11]. Synthesized in both neurons and glia, BDNF plays a multifaceted role, encompassing functions such as the maturation and development of neurons, axonal and neurite outgrowth, neuronal repair, neurotransmitter release or uptake, synapse strengthening, facilitation of long-term potentiation (LTP), regulation of plasticity, and interaction with the inflammation signaling [11, 13, 23]. Neuronal plasticity, a crucial aspect of adaptive neural functioning, enables neurons to respond to new environmental conditions through both functional and structural modifications. However, the disruption of these neuronal functions during conventional whole-brain RT was linked with cognitive dysfunction [7, 35] and demonstrates the importance of BDNF in its pathogenesis. Based on this scientific premise, we hypothesize that RT-induced impairments in neuronal function, elevated neuroinflammation, and cognitive deficits culminate following reductions in neuroprotective BDNF.

The primary rationale for improving in vivo BDNF levels in patients with neurodegenerative conditions such as AD, HD, and MS is to safeguard the brain against substantial structural alterations when exposed to the non-conducive, neurodegenerative environment associated with the disease. In this context, an in vivo increase in BDNF following oral administration of riluzole (RZ) improved cognitive function in a mouse AD model [21]. A comparable approach can be applicable to cancer-related cognitive impairments. Our prior investigations have demonstrated that the oral administration of RZ via drinking water enhanced brain BDNF levels in an animal model subjected to cytotoxic chemotherapy [50]. RZ-mediated increases in BDNF ameliorated chronic chemotherapy (doxorubicin)-induced decline in cognitive function, neurogenesis and prevented neuroinflammation. RZ is an orally bioavailable, and FDA-approved treatment for ALS [55]. In this study, we posit that the administration of RZ will similarly elevate BDNF levels and transcripts, hence protecting the brain from cranial RT-induced synaptic loss and neuroinflammation and improve cognitive function.

Materials and methods

Comprehensive experimental methods, materials, cognitive function, and tissue analysis protocols are provided in the Supplemental Information section.

Animals and RZ treatment

All animal experimentation procedures were ethically approved by the Institutional Animal Care and Use Committee (IACUC) and conducted in compliance with the guidelines established by the National Institutes of Health (NIH). 12–13 weeks old male wild-type mice (C57BL/6) were procured from Jackson Laboratories and were group-housed (four mice per cage) under standard conditions, including a 12 h light–dark cycle, room temperature maintained at 20 °C ± 1, and humidity at 70% ± 10. The mice were provided standard rodent chow diet (Envigo Teklad 2020X) by the University Laboratory Animal Resources (ULAR) at the University of California, Irvine. Previous studies suggested that adult female mice are resistant to acute (9–10 Gy) cranial RT-induced cognitive decline and neuroinflammation [19, 20]. As a proof of principle to support a neurotrophic factor's influence on the damaged, irradiated brain, we focused on male mice for this study. During the first week, mice were anesthetized (5% induction and 2% maintenance isoflurane gas) and cranially irradiated (9 Gy or 0 Gy sham irradiated) using a Small Animal Radiation Therapy (SmART) X-ray irradiator (Precision, Inc., Madison, CT), at a dose rate of 4.91 Gy per minute at 225 keV, and 20 mA. Irradiation was delivered through a 0.3 mm Copper filter and a 10 × 10 mm fixed collimator, with protection to the eyes and cerebellum. Mice were divided into the following groups (N = 12–24 mice/group): Control or irradiated receiving vehicle (Con + Vehicle, RT + Vehicle), or RZ (Con + RZ, and RT + RZ). RZ

(2-amino-6-(trifluoromethoxy) benzothiazole, Selleckchem) was dissolved in filter-sterilized (0.2 µm, Millipore), warm reverse osmosis (RO) water with constant stirring (1–2 h at 45 °C) to achieve a stock concentration of 600 µg/ml [21]. The stock solution was frozen at − 20 °C until usage. The working solution (60 µg/ml) of RZ was prepared twice a week by diluting the stock with filter-sterile RO water. Throughout the study, mice had ad libitum access to either the vehicle (filter-sterile RO water) or Riluzole solution (13 mg/kg per mouse per day, as previously described) [21, 50]. To assess the impact of RZ treatment on in vivo dentate neurogenesis, 2 weeks post-RT, mice were administered BrdU intra-peritoneally (ip, 100 mM, pH 7.6, Sigma) once daily for 6 days.

Cognitive function testing

To investigate the impact of RZ on cognitive function post-RT, mice underwent cognitive assessments and anxiety-related behavioral tests 4 weeks following RZ treatment. Detailed test protocols are available in the Supplemental Information section. The cognitive function tasks, spanning 2–3 weeks, encompassed the open field test (OFT), and elevated plus maze (EPM) for anxiety-like behavior, object location memory (OLM), and a fear extinction memory consolidation task (FE). The OFT task determined the exploration of animals in an open arena to compare the central (60% of central arena) and peripheral zones of the arena. The EPM test assesses an animal's exploration of elevated open arms versus closed (dark) arms in a brightly lit environment. Anxious animals were expected to spend more time in closed arms than open arms. The hippocampal-dependent OLM task evaluated episodic and spatial memory function and gauged an animal's capacity to explore novel object placements in an unconfined, non-invasive open environment (arena) with bedding. The performance on the OLM task is quantified as the Memory Index (MI):

$$MI = \left(\frac{Novel\ exploration\ time}{Total\ exploration\ time}\right) - \left(\frac{Familiar\ exploration\ time}{Total\ exploration\ time}\right) \times 100$$

A positive MI denoted a preference for exploring novel spatial locations, while a negative or zero index indicated little or no preference, with equal or less exploration times for familiar and novel places. Following the completion of the OLM, with an intermission of approximately 72 h, animals were subjected to the FE task. This task aimed to discern the influence of cranial RT or RZ treatment on hippocampal-dependent fear conditioning and the subsequent memory consolidation process (extinction memory), which actively involves dissociating learned responses to past adverse events. Briefly, during the conditioning phase, mice encountered three pairs of evenly spaced auditory stimuli coinciding with a mild foot shock. Twenty-four hours later, across the subsequent 3 days (extinction training phase), animals were exposed to 20 tones within the same contextual environment, including the odor and visual cues. Twenty-four hours after completion of extinction training, the fear test was administered, during which animals encountered three tones in the same context. The freezing behavior of the animals was captured using a ceiling-mounted camera in the FE test chamber and analyzed using an automated freezing measurement module (FreezeFrame, Coulbourn Instruments). The percentage of time each mouse spent freezing during the tone was then calculated for the conditioning, extinction training, and testing phases. For the extinction training phase, an average five tones and four data points per day are presented. Higher the freezing on FE task indicates compromised fear memory consolidation process. The integration of the data from these tests equips us with robust analytical tools for assessing the impact of cranial RT and RZ on cognitive function. Further details of the protocols are provided in the Supplemental Information section.

Immunofluorescence staining, confocal microscopy and immunoreactivity quantification

Following the completion of cognitive function tests, mice were euthanized via intracardiac perfusion using saline with heparin (10 U/ml, Sigma) and 4% paraformaldehyde (PFA) prepared in 100 mM PBS, pH 7.4 (Sigma). Brains were fixed overnight at 4 °C in 4% PFA. Subsequently, tissues were cryo-protected using a sucrose gradient (30%) in PBS supplemented with 0.02% sodium azide (Sigma). Cryo-sectioning was performed using a cryo-stat (HN525 NX, Epredia, Germany) at a thickness of 30 µm (coronal). To investigate the impact of chronic cranial RT and RZ treatments on the neurogenic niche function, serial coronal brain sections (2–3 sections per brain, 8–10 brains per group) through the hippocampal formation were subjected to free-floating immunofluorescence staining using established protocols. Doublecortin (DCX) staining was conducted to label newly born, immature neurons, employing a rabbit anti-DCX primary antibody (1:200; Abcam) and a donkey anti-Rabbit Alexa Fluor 568 secondary antibody. DCX-positive cells were visualized in red using fluorescence microscopy. The BrdU-NeuN dual-immunofluorescence-stained tissues were permeabilized to recover the BrdU antigen and stained with mouse anti-BrdU (1:200) and rabbit anti-NeuN (1:500) primary antibodies. Fluorescence color facilitated using donkey anti-mouse Alexa Fluor 488 (1:200) and donkey anti-rabbit Alexa Fluor 568

(1:500) secondary antibodies. $BrdU^+$ cells were observed in green, and $NeuN^+$ neurons in red. Activated microglia were labeled by IBA1-CD68 dual immunofluorescence staining. Coronal tissues were permeabilized using 0.3% Tween-20 (Sigma) in PBS, followed by treatments with 3% hydrogen peroxide (Sigma) and 10% methanol (Sigma) on ice. Tissues were then blocked with 4% bovine serum albumin (Jackson ImmunoResearch) and 0.3% Tween-20 in PBS, followed by overnight incubation with primary antibodies (rabbit anti-IBA1, 1:500; and rat anti-mouse CD68, 1:500). Fluorescence was developed using goat anti-rat Alexa Fluor 647 (1:1000) and goat anti-rabbit Alexa Fluor 488 secondary (1:500) antibodies. $IBA1^+$ microglia were observed in green, and $CD68^+$ sub-cellular puncta in magenta. To assess synaptic marker, 30-µm-thick sections underwent immunostaining for synaptophysin. Sections were initially washed in PBS (pH 7.4), followed by a 30-min blocking step in 4% (w/v) BSA and 0.1% Triton X-100 (TTX, Sigma). Subsequently, sections were incubated for 24 h in a primary antibody solution containing 2% BSA, 0.1% TTX, and mouse anti-synaptophysin (1:1000). Following primary antibody incubation, sections were treated for 1 h with a solution of goat anti-mouse IgG labeled with Alexa Fluor 647 (1:1000). For NeuN-cFos dual-immunofluorescence staining, 1:500 rabbit anti-cFos and 1:500 mouse anti-NeuN primary antibody solutions made in 3% NDS in Tris-A buffer were used. The secondary antibodies included 1:350 donkey anti-mouse AF 488, and 1:350 donkey anti-rabbit AF 568. After thorough rinsing in PBS, sections were sealed in a *Slow Fade* antifade Gold mounting medium (Life Technologies) for microscopic analysis. Detailed protocols are provided in the Supplemental Information section.

Single (DCX and synaptophysin), and dual (BrdU-NeuN and CD68-IBA1) immunofluorescence-stained sections were imaged using a laser-scanning confocal microscope (Nikon Eclipse AX, Japan) equipped with a 40× oil-immersion objective lens (1.0 NA) and NIS element AR module (v4.3, Nikon). High-resolution (1024–2048 p) z stacks (0.5–1 µm thick) were acquired through the 25–30 µm thick brain sections. Unbiased deconvolution for the fluorescent z stacks and in silico volumetric quantification was carried out as previously described and detailed in the Supplemental Information section. An adaptive 3D blind deconvolution method (ClearView, Imaris v9.2, BitPlane, Inc.) was used to deconvolute and enhance the fluorescence signal resolution with respective fluorescent wavelengths. The deconvoluted images were analyzed using a 3D algorithm-based Imaris module (v9.2). BrdU, and synaptophysin, NeuN, IBA1, and CD68 were 3D modeled using the surface-rendering tool to create individual glial, synaptic, or neuronal cell volume. Using an unbiased, dedicated co-localization channel, the number of $BrdU^+$ cells co-labeled with $NeuN^+$ neurons was individually enumerated. Similarly, IBA1 and CD68 co-localization was determined for activated microglia. The number of DCX^+ cells was quantified using the spot analysis tool. All Imaris-based in silico analyses were conducted using automated batch processing modules, with uniform criteria applied for all experimental groups by an experimenter blinded to the group IDs to avoid bias.

ELISA for BDNF quantification

To assess the impact of RZ on hippocampal BDNF levels, mice subjected to RT ± RZ treatment were euthanized 4 weeks after the initiation of RZ treatment, and BDNF enzyme-linked immunosorbent assay (ELISA) was conducted following established procedures [50]. Brains were promptly extracted from the skull (N = 6–10 mice per group), and the hippocampus was micro-dissected from each cerebral hemisphere. The micro-dissected hippocampi were flash-frozen in cryovials by immersion in liquid nitrogen and stored at − 80 °C until assayed. Each hippocampus was weighed and transferred into 500 µl of ice-cold lysis buffer (NPER, Neuronal Protein Extraction Reagent, ThermoScientific) containing sodium orthovanadate (0.5 mM, Santa Cruz), phenyl-methylsulfonyl fluoride (PMSF, 1 mM, Santa Cruz), aprotinin (10 µg/ml, Santa Cruz), and leupeptin (1 µg/ml; Santa Cruz). Subsequently, tissues were sonicated individually, centrifuged at 4 °C, and the supernatants were collected and diluted at 1:5 or 1:10 with ice-cold Dulbecco's PBS (Gibco). The supernatants were acidified to pH 2.6 and then neutralized to pH 7.6. BDNF levels were quantified using a commercially available ELISA kit (E-EL-M0203, Elabscience Biotechnology) and uncoated ELISA plates (Nunc MaxiSorp, Biolegend). Colorimetric measurements were conducted at a wavelength of 450 nm using a microplate reader (BioTek, SynergyMx).

Spatial transcriptomics, MERFISH

We used a commercial spatial transcriptomics Multiplexed Error-Robust Fluorescence in situ Hybridization (MERFISH) platform (MERSCOPE, Vizgen, Cambridge, MA). MERFISH was performed according to Vizgen's protocol as described previously [27]. Three brain samples, each from the RT + Veh group with the RT + RZ group, were utilized for the MERFISH experiments. Briefly, sagittal cryosections were collected from fresh-frozen OCT-embedded hemibrains of mice examined using a Leica CM1850 cryostat. The sections (10 um) were mounted onto Vizgen merslides (Vizgen #10500001) and hybridized with a specific panel of binary-coded probes that were custom-designed for 500 selected mouse genes (Vizgen #VZG0191, 40 h at 37 °C) after

several steps of pretreatment including fixation (chilled 4% PFA in 1xPBS), permeabilization (70% ethanol), and prehybridization with formamide buffer (Vizgen). After hybridization, the brain sections on merslides were subject to washes with formamide buffer twice (30 min at 47 °C), embedded with polyacrylamide gel, and cleared with a clearing mix containing protease K overnight at 37 °C. Prior to MERFISH imaging, the cleared brain MERFISH samples were stained with DAPI-polyT staining kit included in the MERFISH imaging kit. The MERFISH imaging was conducted with a Vizgen MERSCOPE and a 500-gene imaging kit (Vizgen #10400006) after the merslide was uploaded. Imaging settings were consistent with those previously described [27]. Upon completion of imaging, the MERSCOPE program automatically converted the raw imaging data into.*vzg* meta output files, which were then used for downstream in-depth analysis using our customized bioinformatics pipelines. After analysis, cell-type clusters were identified and annotated, followed by cell-type-specific differential expression analysis using the Wilcoxon rank sum test [53]. Genes were considered significant when the absolute log2 fold change exceeded 0.25 and the adjusted *P* value, calculated using the Benjamini–Hochberg correction method [12], was less than 0.05. To confirm cell type identification, we generated a heatmap displaying expression levels of key marker genes across identified cell types. Each marker gene specific to its cell type was scaled and plotted. This visualization allows clear differentiation of cell types based on characteristic gene expression patterns.

Statistical analysis

All data are expressed as the mean ± SEM. Statistical analyses of cognitive function, biochemical, and immunohistochemical data were conducted using two-way ANOVA (GraphPad Prism, v8.0). For the analysis of irradiation or RZ treatment effects, two-way ANOVA and Bonferroni's multiple comparisons tests were applied. The exploration of familiar versus novel places in the OLM task by the same animals was compared using the Wilcoxon matched-pairs signed-rank test. Fear extinction training data were analyzed using repeated measures ANOVA and Bonferroni's multiple comparisons tests. All statistical analyses were considered significant for a value of $P \leq 0.05$.

Results

Riluzole treatment ameliorates cranial RT-induced cognitive dysfunction

Adult WT male mice received 9 Gy cranial RT and 48 h later administered RZ in drinking water (Fig. 1A). At 1-month post-RZ treatment, mice were handled, habituated, and tested on the cognitive function tasks (Fig. 1B–F). The open field activity of a cohort of animals in the open arena with bedding was monitored. We did not find significant differences in the percentage of time spent in the central zone (60% of the arena) for the spontaneous open field activity (Suppl. Fig. S1A). To determine if cranial RT and RZ treatment affected anxiety-like behavior, animals were administered an elevated plus maze (EPM) task that determines a preference for exploring either elevated open or closed arms of the maze under bright lights. We did not find significant overall group differences between groups for the percentage of time spent in the open arms (Suppl. Fig. S1B). This data indicates the absence of neophobic behavior during the spontaneous exploration cognitive testing. Animals were administered an object location memory (OLM) task to determine hippocampal function. During the OLM test phase, the comparison of the percentage of time animals explored the familiar and novel placements of objects (Fig. 1C) revealed significant differences for the Control + Vehicle, Control + RZ, and RT + RZ groups of mice ($P < 0.0001$, 0.01 and 0.0001, respectively), but not for the RT + Vehicle mice, indicating that irradiated animals receiving vehicle were unable to differentiate between the familiar and novel locations. This behavior for the novel vs familiar location exploration is also reflected in the heat map of animal activity during the OLM test (Fig. 1B). This preference for the novel place exploration was then calculated as the Memory Index (MI). Overall, we found significant group differences between the experimental groups (Fig. 1D, $F_{(3,\ 66)} = 6.43$, $P < 0.001$). Irradiated mice receiving Vehicle (RT + Vehicle) showed a significantly reduced preference to explore the novel location compared to the Control + Vehicle and RT + RZ groups ($P < 0.001$ and 0.01, respectively). Importantly, irradiated mice receiving RZ treatment did not show a reduced MI, and exploration for the novel location was comparable to that of the Control + Vehicle and Control + RZ mice.

Previously, we have shown cranial RT-induced deficits in contextual fear memory and fear extinction memory consolidation [40, 42]. To determine the beneficial neurocognitive impact of RZ, animals were administered the fear extinction memory consolidation task (FE, Fig. 1E). During the conditioning phase (Day 1), all treatment groups showed comparable associative learning as indicated by increased time spent freezing during the tone-shock conditioning phase (Fig. 1E; T_1–T_3; 45–50% on T_3). Twenty-four hours after the conditioning phase, extinction training was administered (Days 1–3). Mice were presented with 20 tones per day (every 5 s intervals) in the same context and odor cue as the conditioning phase, but

without foot shock. The RT + Vehicle group continued to show increased freezing compared to the Control + Vehicle group (Fig. 1E; Extinction Training Day 1–3, *P's* < 0.01). 24 h after the completion of extinction training phase, animals were administered extinction testing (3 tones, 120 s intervals, no foot shock) in the same testing environment that was used for extinction training (Fig. 1F). We found significant group effects in the extinction test (Fig. 1F; $F_{(3, 68)} = 7.79$, $P = 0.0022$). RT + Vehicle mice failed to abolish fear memories during this retrieval testing phase as indicated by the increased freezing levels. On the contrary, RT + RZ mice showed reduced freezing levels compared to RT + Vehicle group (Fig. 1F; $P < 0.0002$). This data indicated that RZ treatment administered to the cranially irradiated animals mitigated impairments in their ability to dissociate the learned response (freezing) to a prior aversive event (the tone-shock pairing). Overall, cognitive function testing demonstrated that RZ ameliorated cranial RT-induced cognitive deficits.

Riluzole treatment augments hippocampal BDNF levels in the irradiated mice

The above cognitive function data indicates a neuroprotective impact of RZ treatment in the irradiated brain. Previously, we have shown RZ-mediated restoration of brain BDNF levels and reversal of cognitive impairments in a chemotherapy-related brain injury model [50]. RZ treatment was also beneficial in a mouse AD model [21]. To link improvements in cognitive function in the irradiated mice receiving RZ, we conducted an ELISA-based quantification of BDNF from the micro-dissected hippocampus. We found a significant overall group effect in the hippocampal BDNF levels (Fig. 2; $F_{(3, 26)} = 8.61$, $P < 0.001$). Cranial RT (RT + Vehicle) was associated with 50–53% decrease in the BDNF levels compared with either Control + Vehicle ($P < 0.005$) or Control + RZ ($P < 0.02$) groups. RZ treatment significantly increased hippocampal BDNF levels in the irradiated mice ($P < 0.05$) compared to RT + Vehicle group. Thus, we posit that RZ treatment augmented BDNF in the irradiated brain that potentially contribute to cognitive recovery.

BDNF enhancement restores cranial RT-induced synaptic loss

Our past work has shown cranial RT-induced loss of synaptic integrity including pre- and post-synaptic proteins that leads to long-term cognitive impairments [40, 42]. BDNF plays an important role in preserving neuronal function, including the synaptic landscape. To determine the impact of RZ treatment and BDNF augmentation on synaptic integrity in the irradiated brain, we quantified immunoreactivity of a synaptic marker, synaptophysin (Fig. 3). We found a significant overall group effect in the molecular layer ($F_{(3, 28)} = 4.002$, $P < 0.02$) and stratum radiatum ($F_{(3, 28)} = 19.32$,

(See figure on next page.)

Fig. 1 Treatment with riluzole reverses cranial radiation-induced cognitive impairments. **A** Research design: 12–13 weeks old wild type (C57BL/6) male mice received cranial radiation therapy (RT, 0 or 9 Gy) with protection of eyes and cerebellum. 48 h after cranial RT, mice were treated with riluzole (RZ) in the drinking water (13 mg/kg) and continued on RZ till the end of the study (6–7 weeks). 0 Gy irradiated animals that received drinking water served as the vehicle group. For the assessment of dentate neurogenesis, 2 weeks post-RT, mice received BrdU injections (5-Bromo-2′-deoxyuridine, 50 mg/kg, IP, once daily for 6 days). One month after initiation of RZ treatment, mice were administered a hippocampal-dependent spatial memory retention test (Object Location Memory, OLM), anxiety-related tasks (Open Field Activity, OFT; and Elevated Plus Maze, EPM), and in the end, a fear extinction memory consolidation task (FE). After completion of cognitive testing, mice were euthanized, and brains were collected for the tissue analyses. **B** Representative heat maps depicting animals exploring novel or familiar placement of objects in each experimental group during the OLM task. **C** Cranially irradiated mice receiving vehicle spent significantly less time exploring the novel placement of the object. Percentage time spent exploring the novel placements of objects during the test phase of the OLM task show that Control + Vehicle, Control + RZ and RT + RZ mice spent significantly more time exploring novel versus familiar location whereas RT + Vehicle group spent comparable time exploring both locations indicating a novel place location memory deficit. **D** For the OLM task, the tendency to explore a novel placement of the object was derived from the Memory Index (MI), calculated as ([Novel location exploration time/Total exploration time]—[Familiar location exploration time/Total exploration time]) × 100. Cranial RT significantly impaired spatial location memory as indicated by significantly reduced MI in the RT + Vehicle group compared to the Control + Vehicle, and RT + RZ group. Importantly, irradiated mice treated with RZ did not show a decline in spatial location memory and the MI was significantly higher compared to the RT + Vehicle group. **E** During the conditioning phase fear extinction memory task, cranial RT or RZ treatment did not impair the acquisition of conditioned fear response as indicated by the elevated freezing following a series of three-tone and shock pairings (80 dB, 0.6 mA, T1–T3). 24 h later, fear extinction training was administered every 24 h (20 tones) for the subsequent 3 days. Each data point for the extinction training Days 1–3 is presented as average of percentage time freezing for 5 tones (4 data points per day). All group of mice showed a gradual decrease in freezing behavior (Days 1–3), however, RT + Vehicle group spent a significantly higher time freezing compared with Control + Vehicle group. **F** Twenty-four hours after the extinction training phase, on the extinction test, Control + Vehicle and Control + RZ mice showed abolished fear memory (reduced freezing) compared with the RT + Vehicle mice. Importantly, cranial RT-exposed mice receiving RZ (RT + RZ) were able to successfully abolish fear memory (reduced freezing) compared with the RT + Vehicle group. Data is presented as mean ± SEM ($N = 10$–26 mice per group). *P* values were derived from two-way ANOVA and Bonferroni's multiple comparisons test. *$P < 0.01$, versus Control + Vehicle. **$P < 0.0001$, T1 versus T3 for all experimental groups

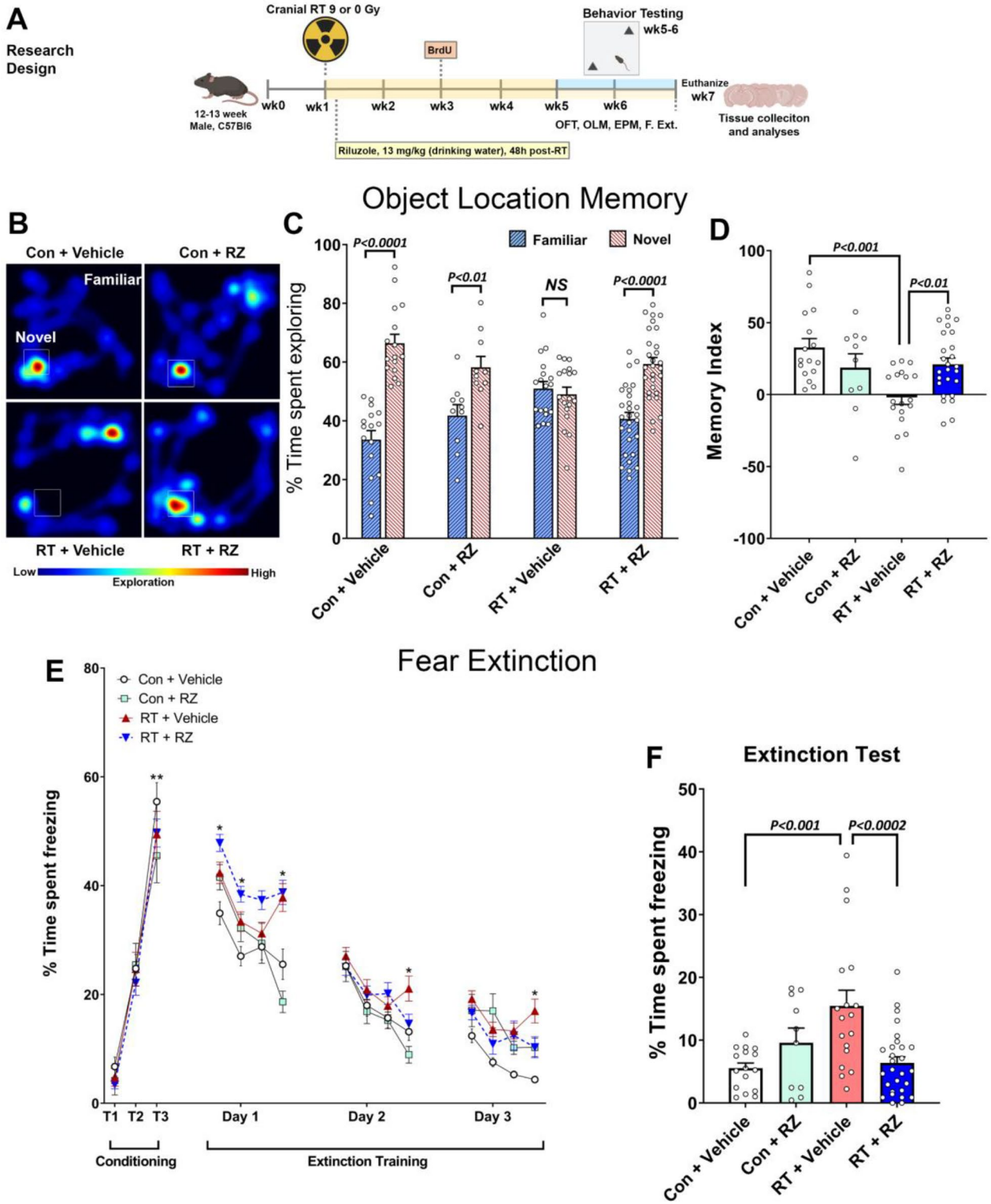

Fig. 1 (See legend on previous page.)

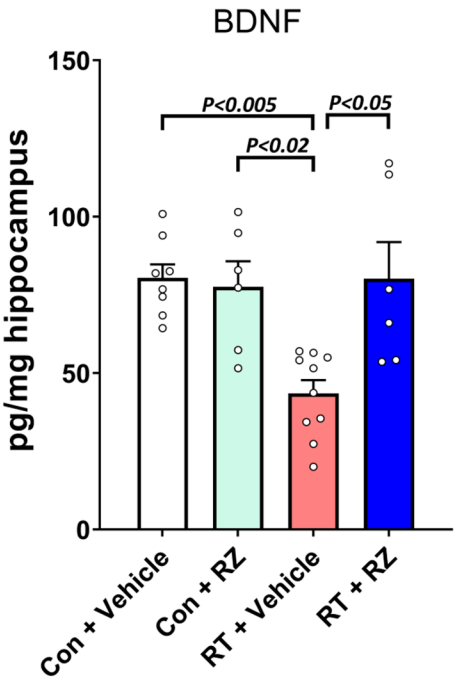

Fig. 2 Riluzole treatment restores hippocampal BDNF in the irradiated hippocampus. 10–12 weeks old WT male mice received cranial radiation therapy (RT) followed by riluzole (RZ) treatment (13 mg/kg) in drinking water for 6–7 weeks. An ELISA-based quantification of BDNF from the micro-dissected hippocampus showed RT-induced reductions in the RT + Vehicle group. Importantly, RZ treatment in the cranially irradiated mice showed significant restoration of BDNF levels. Data are presented as mean ± SEM ($N = 6–10$ mice per group). *P* values were derived from two-way ANOVA and Bonferroni's multiple comparisons test

$P < 0.0001$) for synaptophysin immunoreactivity. Cranial RT significantly reduced synaptophysin$^+$ immunoreactive puncta compared to the Control + Vehicle group in the hippocampal dentate gyrus molecular layer ($P < 0.04$, Fig. 3A, B) and CA1 stratum radiatum ($P < 0.0001$, Fig. 3C, D). The synaptophysin levels were comparable between the Control + Vehicle and Control + RZ groups. Irradiated mice receiving RZ treatment did not show reduced synaptophysin compared to the RT + Vehicle group in the molecular layer ($P < 0.04$) and stratum radiatum ($P < 0.001$). Overall, this data indicates a protective role of RZ treatment and BDNF restoration against RT-induced disruption of synaptic loss.

BDNF augmentation remediates cranial RT-induced reduction in neuronal plasticity

To further determine the impact of RZ treatment and BDNF restoration in the irradiated brain on neuronal function, we evaluated the neuron plasticity-related immediate early gene (IEG) product, cFos, co-stained with the mature neuronal marker, NeuN, in the hippocampal dentate gyrus granule cell layer (GCL, Fig. 4). cFos facilitates neuronal LTP and hippocampal-dependent memory formation. A significant overall group effect was found in the number of cFos-NeuN$^+$ dual-labeled cells ($F_{(3,\ 26)} = 4.68$, $P < 0.01$). We found significantly reduced neuronal cFos (cFos-NeuN$^+$) in the RT + Vehicle group compared to Control + Vehicle group ($P < 0.02$, Fig. 4A–D) indicating compromised mature neuronal plasticity. Conversely, treatment with RZ significantly restored the number of cFos-NeuN$^+$ cells in the irradiated GCL (Fig. 4A, E). This data in conjugation with synaptic protein expression data (Fig. 3) indicated restorative effects of RZ treatment in the irradiated brain.

Riluzole treatment did not reverse cranial RT-induced decline in neurogenesis

In our past study using a chemotherapy-induced cognitive impairment model, RZ treatment reversed chemotherapy-induced loss of newly born neurons and neurogenesis. Cranial RT has been shown to impact neural progenitor cell (NPC) function with an overall decline in doublecortin$^+$ (DCX) newly born neurons and mature neurons differentiated from NPC pools in the hippocampal sub-granular zone (SGZ) [6, 8, 46]. We quantified DCX$^+$ fluorescence neurons in the hippocampal GCL and SGZ. A significant overall group difference was found for the number of DCX$^+$ immature neurons (Fig. 5A–E; $F_{(3,\ 24)} = 255.5$, $P < 0.0001$). Cranial RT significantly reduced the number of DCX$^+$ cells in hippocampal GCL and SGZ compared to either Control + Vehicle and Control + RZ groups (Fig. 5E, $P < 0.001$). Treatment with RZ did not mitigate the loss of DCX$^+$ immature neurons in the irradiated hippocampus. Furthermore, we quantified the impact of RZ treatment on the dentate neurogenesis post-RT. Two weeks post-RT (Fig. 1A), mice were treated with BrdU to label proliferating NPCs. The assessment of neurogenesis (BrdU$^+$-NeuN$^+$ dual-labeled cells) was conducted 6–7 weeks later. We found overall significant effects on the percentage of BrdU$^+$ cells expressing NeuN (Fig. 5F–J, $F_{(3,\ 51)} = 70.22$, $P < 0.0001$). Cranial RT (RT + Vehicle) significantly reduced the percentage BrdU$^+$-NeuN$^+$ cells compared with Control + Vehicle and Control + RZ groups (Fig. 5J, $P < 0.001$). Treatment with RZ did not restore BrdU$^+$-NeuN$^+$ cells in the RT + RZ hippocampus. This data indicates that in the irradiated microenvironment, treatment with RZ was ineffective in restoring neurogenesis.

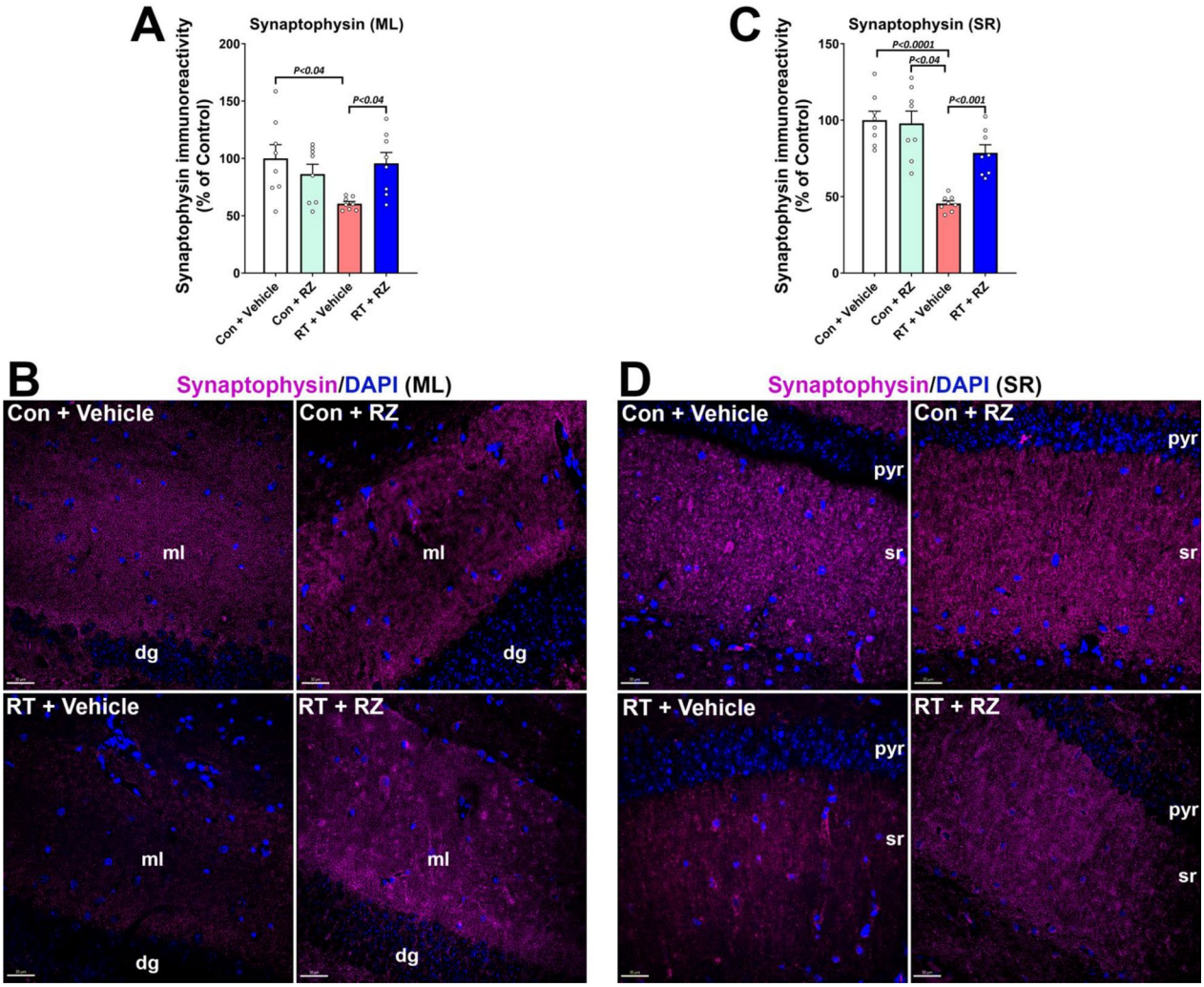

Fig. 3 Riluzole treatment reverses cranial radiation-induced synaptic loss. Adult male mice were exposed to cranial RT and 48 h later received riluzole (RZ, 13 mg/kg) in drinking water for 6–7 weeks. Synaptic protein marker, synaptophysin, in the molecular layer (*ml*) of hippocampal dentate gyrus (*dg*, **A**, **B**) and CA1 stratum radiatum (*sr*, **C**, **D**) emanating from the pyramidal neuron layer (*pyr*) was quantified using immunofluorescence staining, confocal microscopy and 3D algorithm-based unbiased fluorescent puncta analysis of synaptophysin immunoreactivity (magenta; DAPI nuclear stain, blue). Cranial RT (RT + Vehicle) significantly reduced the synaptophysin immunoreactivity in the *dg ml*, and CA1 *sr* regions compared with Control + Vehicle group. Irradiated mice receiving RZ showed a significantly increased synaptophysin immunoreactivity compared with the RT + Vehicle group. Data ise presented as mean ± SEM ($N = 8$ mice per group). *P* values were derived from two-way ANOVA and Bonferroni's multiple comparisons test. Scale bars, 30 µm, (**B**, **D**)

Riluzole treatment reduces cranial RT-induced neuroinflammation

Our previous studies using chemotherapy and cranial RT rodent models [1, 2, 4, 5, 9, 14, 40, 42], have shown elevated neuroinflammation; particularly microglial activation and astrogliosis in the brain, linked with cognitive decline. In addition, we have shown that RZ treatment reduced microglial activation in the chemotherapy-exposed brain in vivo [50]. Thus, to assess the effectiveness of RZ treatment on the status of microglial activation in the RT brain, dual immunofluorescence staining (Fig. 6A–C, and a1) and 3D algorithm-based volumetric analysis (Fig. 6A) was conducted for a pan microglial marker (IBA1) and a phagocytosis lysosomal marker (CD68). We found a significant overall group effect in microglial activation (IBA1-CD68 dual-immunoreactivity, $F_{(3, 24)} = 12.95$, $P < 0.001$). Exposure to cranial irradiation significantly elevated IBA1-CD68 co-labeling in the hippocampus (RT + Vehicle, Fig. 6A) compared to Control + Vehicle ($P < 0.03$) and Control + RZ ($P < 0.001$) groups. Cranial RT also elevated astrocytic hypertrophy (astrogliosis) as indicated by thicker and longer

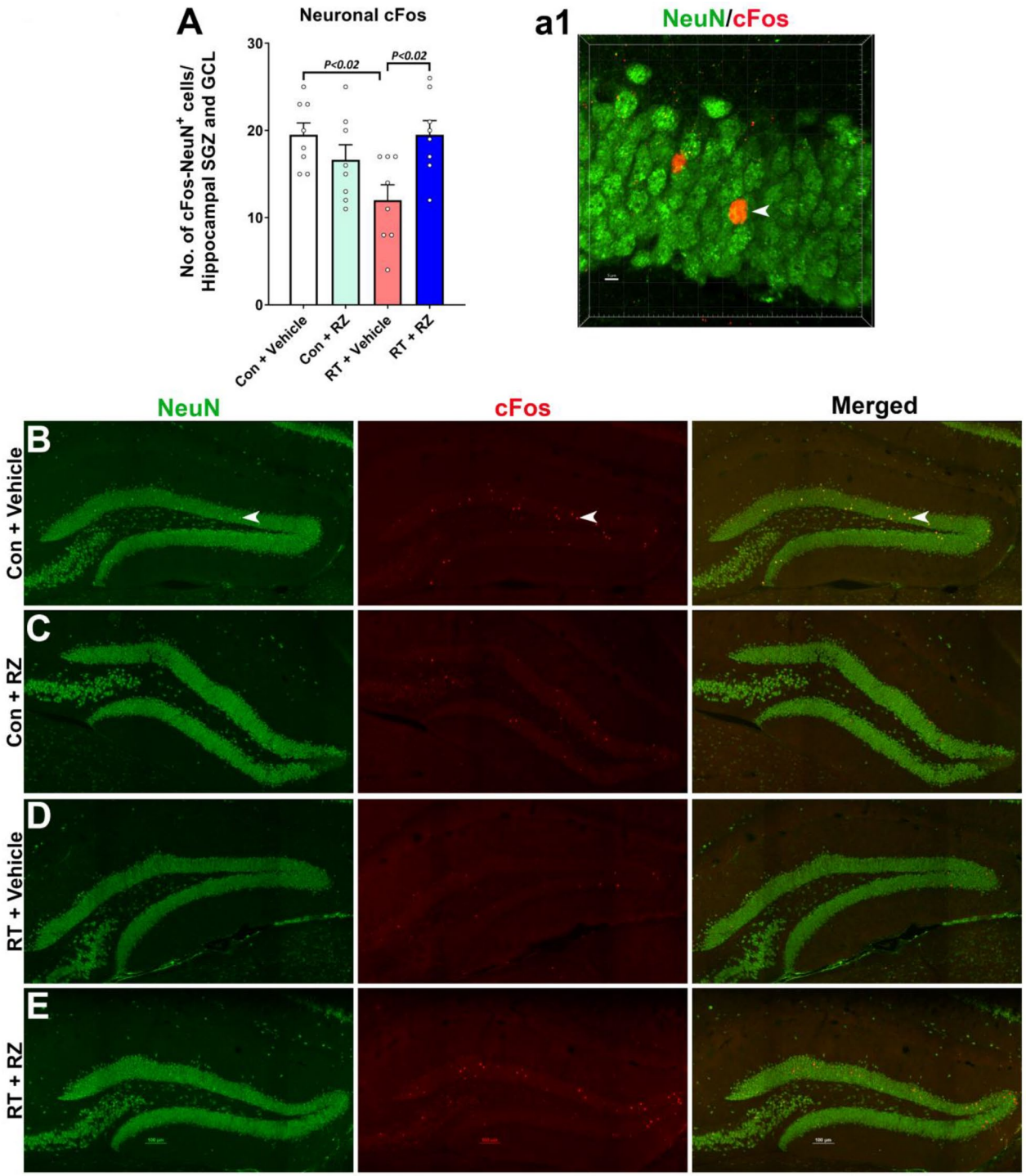

Fig. 4 Treatment with riluzole prevents cranial radiation-induced reduction in the neuronal plasticity-related cFos expression. **A**, **a1** Dual immunofluorescence staining, confocal microscopy and 3D algorithm-based unbiased quantification of NeuN$^+$ (green) neuronal plasticity-related immediate early gene (IEG) expression product, cFos showed a significant reduction in the number of cFos-NeuN$^+$ neurons in the irradiated (RT + Vehicle) hippocampal sub-granular zone (SGZ) and the granule cell layer (GCL) compared to Control + Vehicle group. **B**–**E** Single channel fluorescent z stacks for NeuN (green), cFos (red) and merged images show cFos-NeuN co-expression in the hippocampal dentate gyrus for each treatment group. **a1** Higher magnification 3D fluorescent z stack of dual-stained neuron (arrow) is shown for the Control + Vehicle group **B**. Treatment with riluzole significantly increased the number of cFos-NeuN$^+$ neurons in the irradiated hippocampus (RT + RZ) compared to irradiated mice receiving vehicle (RT + Vehicle). Data is presented as mean ± SEM ($N = 8$ mice per group). *P* values were derived from two-way ANOVA and Bonferroni's multiple comparisons test. Scale bars, 100 µm, (**B**–**E**), and 5 µm, (**a1**)

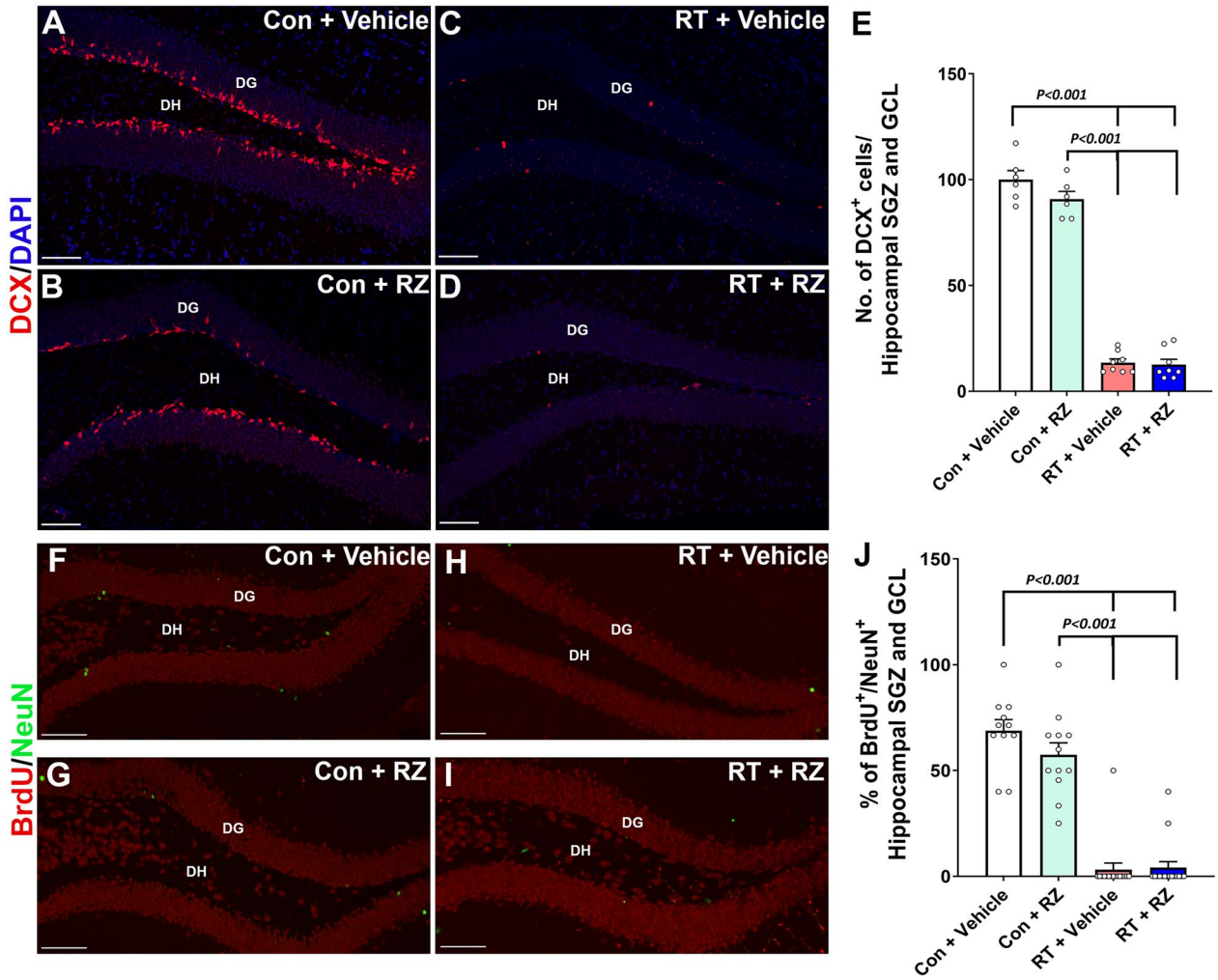

Fig. 5 Riluzole treatment did not prevent cranial radiation-induced decline in neurogenesis. WT adult male mice received cranial RT (9 Gy) and treated with riluzole (RZ, 13 mg/kg) 48 h later in their drinking water for 6–7 weeks. Two weeks post-RT, mice were treated with BrdU and hippocampal neurogenesis was quantified using newly born neuron marker, doublecortin (DCX), and BrdU-NeuN dual-immunofluorescence staining in the hippocampal dentate gyrus (DG) sub-granular zone (SGZ) and molecular layer (ML) 6-7 weeks after the BrdU treatment. Cranial RT (RT + Vehicle) significantly reduced the number of DCX^+ neurons (red, **A**–**D**) in the hippocampus compared with either Control + Vehicle or Control + RZ groups **E**. RT also significantly reduced neurogenesis, as indicated by the reduced percentage of $BrdU^+$ cells (red) differentiating into the mature neurons (green, NeuN; **F**–**I**) in the RT + Vehicle group compared with either Control + Vehicle or Control + RZ groups (**J**). Riluzole treatment to the irradiated animals did not prevent the loss of DCX^+ newly born neurons and the decline in dentate neurogenesis ($BrdU^+$-$NeuN^+$ dual-fluorescent cells). Data is presented as mean ± SEM ($N = 6$–16 mice per group). *P* values were derived from two-way ANOVA and Bonferroni's multiple comparisons test. Scale bars, 50 µm, (**A**–**D**) and (**F**–**I**)

stelae and GFAP immunoreactivity (Suppl. Fig. S2) in the RT + Vehicle group compared to Control + Vehicle and Control + RZ groups ($P < 0.001$, Fig. 6D, E). The overall group difference was significant for GFAP immunoreactivity ($F_{(3, 28)} = 22.08$, $P < 0.0001$). On the other hand, RZ treatment to the irradiated mice (RT + RZ) significantly reduced activated microglia (IBA1-CD68; Fig. 6A) and astrogliosis (GFAP; Fig. 6D) compared to the RT + Vehicle group ($P < 0.001$, *and* $P < 0.0001$ respectively). This data signifies the neuroprotective impact of RZ treatment in the irradiated brain leading to reductions in gliosis and cognitive dysfunction.

Riluzole treatment improves transcriptomic signatures against cranial RT-induced neurodegeneration

For this study, we utilized MERFISH to perform spatial transcriptomics profiling of individual brain sections, with a specific focus on the hippocampal brain region [27, 57, 58]. Through the bioinformatics analysis platform, we collected about 6000 brain cells and identified 10 major

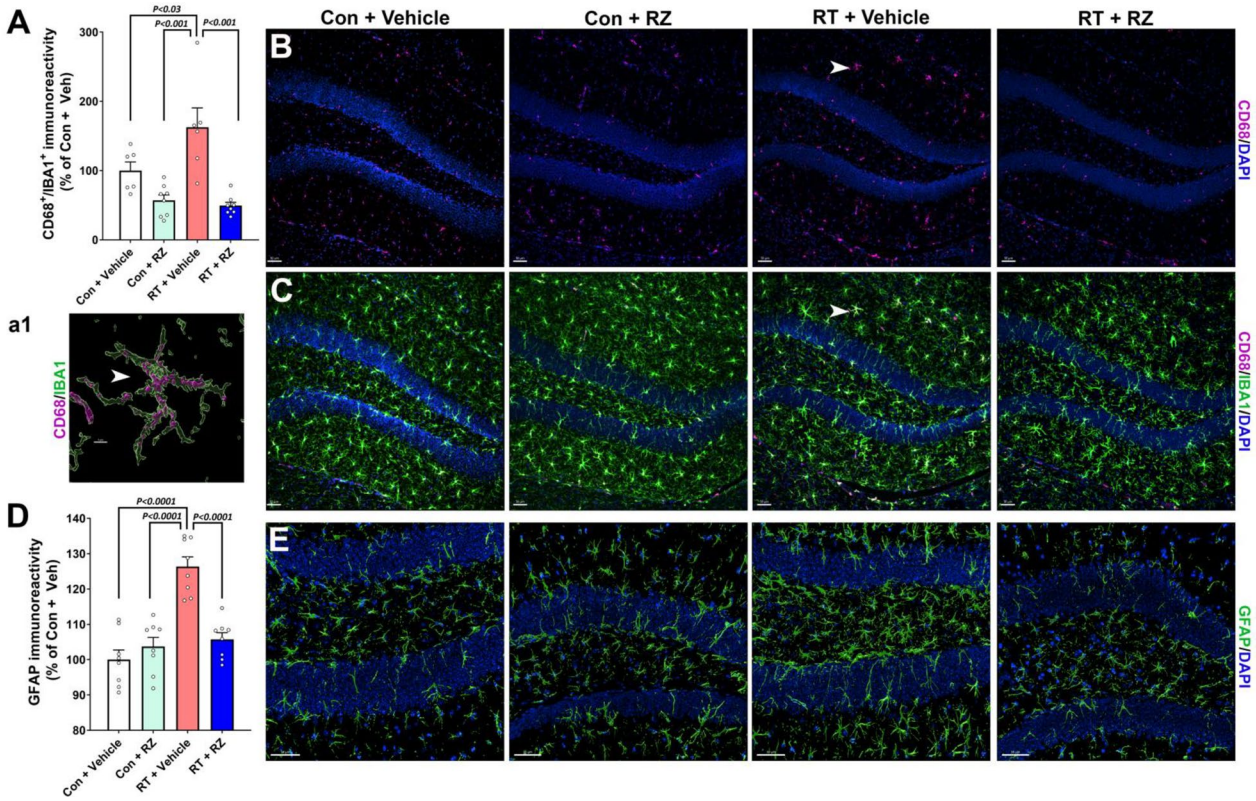

Fig. 6 Riluzole treatment reduces cranial radiation-induced glial activation. Radiation-induced activated microglia in the hippocampal granule cell layer (GCL) and dentate hilus (DH) were assessed using dual immunofluorescence staining, laser scanning confocal microscopy and 3D algorithm-based volumetric quantification for IBA1 (green) and CD68 (magenta, and DAPI, blue) dual-labeling. **A**–**C** Exposure to cranial irradiation (RT + Vehicle) significantly elevated the immunoreactive volume of activated microglia ($CD68^+$-$IBA1^+$ co-localization) in the hippocampus compared with either Control + Vehicle or Control + RZ groups. Irradiated mice receiving RZ (RT + RZ group) showed a significantly reduced volume of $CD68^+$-$IBA1^+$ co-labeling compared with the RT + Vehicle group. CD68 alone (**B**) and CD68-IBA1 merged **C** fluorescence channels are shown for each group. **a1** Higher magnification surface reconstruction for the $IBA1^+$ (green) positive microglia expressing CD68 puncta (magenta) is shown for the selected cell (white arrow, **B**, **C**) from the RT + Vehicle group. **D**–**E** Surface reconstruction of $GFAP^+$ (green, DAPI, blue) hippocampal astrocytes shows significantly elevated GFAP immunoreactivity volume in the RT + Vehicle group compared to either Control + Vehicle or Control + RZ group. Astrocytes showed hypertrophy with thicker and longer stelae in the irradiated hippocampus (RT + Vehicle). RZ administration to the irradiated mice (RT + RZ) showed a significant reduction in astrogliosis compared to RT + Vehicle group. Volumetric data for $CD68^+$-$IBA1^+$ co-expression and GFAP immunoreactivity are presented as mean ± SEM ($N = 6$–8 mice per group). *P* values were derived from two-way ANOVA and Bonferroni's multiple comparisons test. Scale bars, 30 µm, (**B**), 5 µm, (**a1**), and 50 µm, (**E**)

cell types, including excitatory neurons from the CA1, CA3, and dentate gyrus regions, as well as glial cells including astrocytes and microglia within the hippocampus (Fig. 7A, B). Cell type identification was verified using marker genes (Fig. 7C). Significant changes in the gene expression comparing Con + RZ with Con + Vehicle (Suppl. Table T1), RT + Vehicle with Con + Vehicle (Suppl. Table T2), and RT + RZ with RT + Vehicle (Suppl. Table T3) are provided in the Supplemental Information. Our dataset, which contains spatial locations and gene expression profiles of individual cells, including BDNF-related genes, combined with annotated cell types, offers a unique opportunity to explore the spatial *bdnf* and other gene expression in the intact tissue context. In the comparison of the RT + Veh with RT + RZ groups, we observed a significant increase in the *bdnf* gene expression in hippocampal excitatory neurons in the RZ-treated group (Fig. 7D-E, Wilcoxon Rank Sum test, average log2-fold change = 0.31, FDR-adjusted $P < 0.0001$). In a comparison of the Con + Vehicle and RT + Vehicle groups, we observed a significant decrease (average log2-fold change = − 0.35, FDR-adjusted $P < 0.00001$) in *bdnf* expression in hippocampal excitatory neurons in the RT + Vehicle group. Additionally, comparing the Con + Vehicle with Con + RZ groups revealed no significant change in *bdnf* expression in hippocampal excitatory neurons (average log2-fold change = − 0.16, FDR-adjusted $P \approx 1$, Fig. 7F-G). Importantly, we found

upregulated expression of an IEG, *nptx1*, which is known to play a role in synaptic plasticity and neuroprotection, in the hippocampal excitatory neurons in the RT + RZ group compared to RT + Veh group (Wilcoxon Rank Sum test, average log2-fold change = 0.27, FDR-adjusted $P < 10^{-16}$). These findings suggest that RZ treatment counteracts cranial RT-induced neurodegeneration by enhancing neuroplasticity and neuroprotection in the hippocampus through the upregulation of key immediate early genes in excitatory neurons.

Discussion

This study verifies the neuroprotective role of riluzole treatment-mediated in vivo BDNF enhancement against cranial RT-induced cognitive dysfunction. Importantly, oral administration of RZ in the cranially irradiated mice minimized the RT-induced loss of synaptic integrity and neuronal plasticity and reduced neuroinflammation, hallmarks of radiation-induced long-term neurodegenerative consequences leading to cognitive decline. These results also corroborate our past findings showing the reversal of cognitive impairments and neurodegeneration in chemotherapy-induced brain injury [50]. A likely common mechanism in each of these neurodegeneration and cognitive decline models was the reduction in BDNF. RZ treatment restored the neuronal BDNF in vivo, which played a contributory role in cognitive recovery in the irradiated brain.

Our hypothesis that enhancing levels of a neurotrophic factor in the irradiated brain would improve cognitive function is based on the scientific premise showing a correlation between BDNF levels and brain function. Behavioral deficits observed one month following a 30 Gy acute high-dose cranial RT were correlated with significantly reduced *bdnf* transcripts and protein expression [25]. These decrements in BDNF were linked with *bdnf* gene promoter histone H3 acetylation, a gene silencing epigenetic modification, in the irradiated hippocampus. Cranial RT doses of 5–10 Gy also downregulated BDNF mRNA, protein, and pCREB levels, phosphorylated cAMP-response element binding protein, in the irradiated hippocampus that was linked with hippocampal-dependent learning and memory deficits. Phosphorylation of CREB, a leucin-zipper class transcription factor, plays important roles prior to the transcription of neurotrophins (NTs) including BDNF and NT3 in hippocampal granule cell neurons [48]. Conversely, neuroprotective effects of BDNF-mediated cognitive recovery in a 20 Gy acute cranial RT model were blocked following treatment with a tyrosine kinase inhibitor that disrupts BDNF signaling [47]. These reports link cranial RT and the downregulation of BDNF expression and signaling impacting cognitive function. Interestingly, forced wheel running exercise following 20 Gy acute RT in rats improved cognitive function, neurogenesis and BDNF expression in vivo [24]. Physical exercise has also been shown to improve cognitive function following chemotherapy in animals [54]. Physical activities, including running, have been shown to be linked with increased brain BDNF levels that improve neuronal plasticity [51]. Collectively, these studies support an overall strategy for enhancing BDNF in vivo to improve cognitive function following cytotoxic cancer therapies. A number of studies also suggest a positive correlation between improved cognitive indices and BDNF in cancer patients undergoing chemotherapy [44], thus supporting our hypothesis that in vivo BDNF enhancement is neuroprotective against cranial RT-induced cognitive decline.

BDNF has been shown to play neuroprotective and functional roles in maintaining neuronal and dendritic health, activity-dependent neuronal plasticity, and cognitive function [30, 38]. Reduced serum BDNF levels were associated with mild cognitive impairments, AD, and depression-related disorders [11]. Relatively higher expression of BDNF in the hippocampus has been linked with hippocampal-dependent cognitive function, synaptic plasticity, and maintenance of neurogenesis [38]. Our past studies using cancer therapy-related cognitive impairment (CRCI) models demonstrated that exposure to either acute or fractionated RT and cytotoxic

(See figure on next page.)

Fig. 7 Spatial transcriptomic analysis of the cell-type-specific gene expression in the irradiated brain reveals upregulation of *bdnf* and *nptx1* in hippocampal excitatory neurons following riluzole treatment. **A** Spatial distribution plot of the hippocampus region in an individual brain section from the RT + Veh group, showing the localization of major cell types in MERFISH spatial transcriptomics profiling. **B** The UMAP visualization of 10 major cell types identified within the hippocampus, including excitatory neurons from the CA1, CA3, and dentate gyrus (DG) regions, inhibitory neurons, and non-neuronal (glial) cells including astrocytes (AST), microglia (Mic), oligodendrocyte granule cell and precursor cell (OGC, OPC), pericyte (Peri), endothelial cells (Endo). **C** Heatmap of marker gene expression for cell type identification. **D** Volcano plot illustrating differentially expressed genes between RT + RZ and RT + Veh groups in hippocampal excitatory neurons, highlighting the significant upregulation of *bdnf* and *nptx1*. **E** Violin plot showing the increased expression of *bdnf* in hippocampal excitatory neurons of the RT + RZ group compared to the RT + Veh group. The expression values were log-normalized. **F**, **G** Volcano plots of differentially expressed genes in hippocampal excitatory neurons between RT + Veh and Con + Veh, and Con + Rz and Con + Veh groups, serving as control comparisons to validate findings in (**D**). *P* values were derived from Wilcoxon Rank Sum test and adjusted by Benjamini–Hochberg methods. Scale bar, 0.5 mm, (**A**)

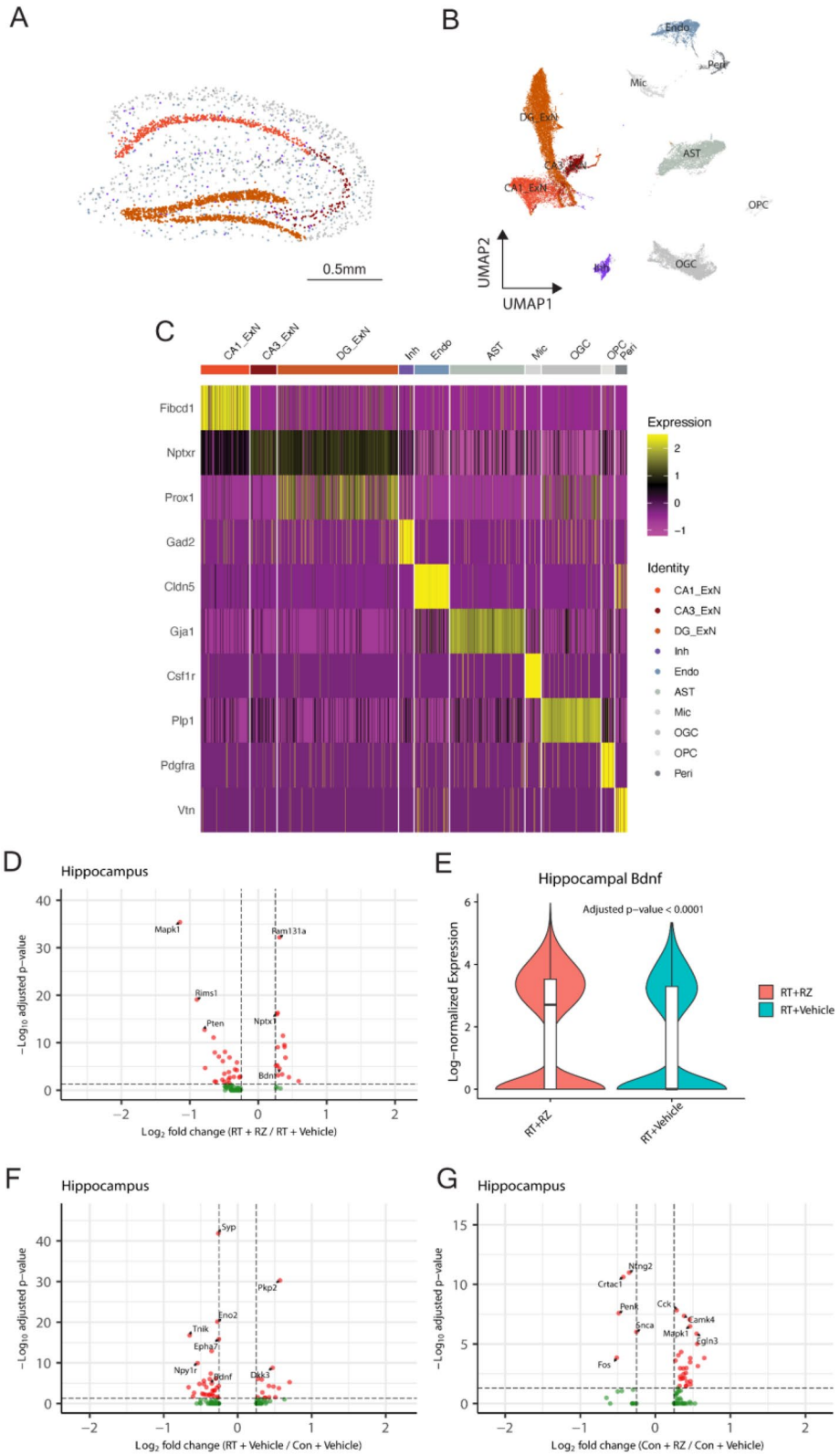

Fig. 7 (See legend on previous page.)

chemotherapy using drugs such as cyclophosphamide or doxorubicin significantly impaired dentate neurogenesis and cognitive function [6, 8, 14, 29, 33, 46]. Treatment with RZ in doxorubicin-exposed mice restored DCX^+ newly born neurons and neural progenitor cell (NPC)-derived mature neurons [50]. Conversely, in this study, RZ treatment and BDNF enhancement did not reverse RT-induced loss of neurogenesis (Fig. 5). Thus, RZ treatment-related improvements in cognitive function in the irradiated animals were unrelated to neurogenesis. These results led us to conduct in depth, cell type-specific transcriptomic profiling (MERFISH, Fig. 7) of the irradiated hippocampus. We found elevated expression of genes associated with synaptic plasticity (NPTX1), synaptogenesis (NRG2), and neurotrophins (BDNF, NT3) in the excitatory neurons in the irradiated brain treated with RZ compared to irradiated mice receiving vehicle. We also analyzed a pre-synaptic protein, synaptophysin, and a neuronal plasticity-related IEG product, cFos, expression in the irradiated hippocampus. Exposure to cranial RT significantly reduced synaptophysin in the dentate molecular and CA1 stratum radiatum layers (Fig. 3). Our past studies using pre-clinical CRCI models have established that exposure to cranial RT, cytotoxic chemotherapy using cyclophosphamide or doxorubicin, and immune checkpoint inhibition therapy reduced hippocampal synaptic density that was associated with cognitive impairments [3, 5, 22, 29, 40, 42, 50]. Importantly, we also found significant reductions in IEG expression, including the neuronal cFos in the irradiated hippocampus (Fig. 4). cFos, similar to pCREB, facilitates hippocampal neuronal plasticity and LTP, glutamatergic receptor activity and memory function [28]. Conversely, treatment with RZ and in vivo increase in the BDNF, and NT3 by the excitatory neurons ameliorated RT-induced loss of synaptic integrity and neuronal IEG expression (Figs. 4, 7). Concurrently, using spatial transcriptomic profiling of hippocampus derived from the irradiated mice receiving RZ treatment, we found 15 upregulated and 28 downregulated genes. Amongst those elevated was *nptx1* gene expression within the excitatory neurons compared to irradiated mice receiving vehicle (RT + Vehicle, Fig. 7). NPTX1, neuronal pentraxin, is a crucial pre-synaptic class protein shown to facilitate synaptic strengthening, plasticity, and resilience in vivo [16]. Loss of NPTX1 led to cognitive impairments in neurodegenerative conditions. We also found upregulation of NRG2 and NT3 genes in the RT + RZ group compared to RT + Vehicle group. NRG2 (neuregulin 2) expression is abundant in the hippocampal DG and plays an important role in synaptogenesis [37]. NRG2 facilitates glutamatergic synapse maturation and dendritic growth [31]. Moreover, NRG2 directly impacts the survival of oligodendrocytes and its progenitors [10]. NT3, similar to BDNF, is a neurotrophic factor and plays an important role in neuronal development, synaptogenesis, and synaptic plasticity [36, 49]. The prominent role of NT3 in LTP and synaptic plasticity maintenance has been demonstrated in Huntington's disease model [15]. Collectively, this data supports the neuroprotective role of RZ treatment and BDNF augmentation in preserving mature, excitatory neuronal function in the irradiated brain and, thereby, cognitive recovery.

Our past pre-preclinical studies have shown cranial RT-induced microglial activation, astrogliosis, and elevated hippocampal cytokines (TNFa, IL1b, IL-6, IL-1a) that led to excessive synaptic loss and cognitive dysfunction [29, 40]. Our clinical studies of cancer patients undergoing chemotherapy found a correlation between pro-inflammatory signaling via TNFa, reduced plasma BDNF, and persistent cognitive impairments [44, 45], pointing to a neuro-modulatory role of inflammation and BDNF. Neurodegenerative condition-related neuroinflammation has been linked with the downregulation of the protective BDNF signaling [34]. In this study, we found reductions in the RT-induced hippocampal microglial activation and astrogliosis following RZ treatment and in vivo BDNF augmentation. Together, this data suggests that RZ treatment-related reductions in neuroinflammation in the irradiated brain contributed to preventing excessive synaptic and neuronal plasticity loss and cognitive decline.

While we have not evaluated these possibilities yet, we acknowledge that in addition to enhancing BDNF in vivo (as shown by ELISA, Fig. 2; and transcriptomics, Fig. 7), neuroprotective effects of RZ treatment can also positively impact other neural functions, including increasing LTP, reducing neuronal glutamate release, increasing glial glutamate reuptake, and inhibiting glutamatergic receptor activity that may influence irradiated brain function. Other reports demonstrating the beneficial effects of RZ on the AD brain have shown reduced neuronal glutamate release and amelioration of long-term memory deficits in AD mouse models. [18, 32] In vitro experiments using primary mouse astrocytes showed a two to threefold increase in BDNF, GDNF (glial cell line-derived neurotrophic factor), and NGF (nerve growth factor) synthesis 24 h after initiation of RZ treatment [41]. Thus, both neurotrophic and neuronal mechanisms may contribute to the beneficial neurocognitive impact of RZ on the irradiated brain.

The overarching goal of our approach is to test this clinically-relevant, and translationally feasible, orally available, pharmacologic strategy in brain cancer-bearing mouse models receiving fractionated cranial RT and chemotherapy (*e.g.* temozolomide) regimes to expand the prospect of RZ treatment to ameliorate cognitive decline

in cancer survivors and improve their quality of life. The future pre-clinical and clinical testing should also verify that treatment with RZ is safe in cancer-bearing subjects, and it does not interfere with therapeutic efficacy of cranial RT to thwart brain cancers. Nonetheless, this study provides *proof of concept* that in vivo augmentation of BDNF via oral administration of RZ in radiotherapy-injured brain is neuroprotective.

Conclusion

Our data provides pre-clinical evidence for a translationally feasible approach: oral administration of an FDA-approved compound, riluzole, to enhance BDNF in vivo to ameliorate cranial radiation therapy-induced adverse impact on synaptic integrity, neuronal plasticity, neuroinflammation, and cognitive function.

Abbreviations

AD	Alzheimer's disease
ALS	Amyotrophic lateral sclerosis
ANOVA	Analysis of variance
BDNF	Brain-derived neurotrophic factor
BrdU	5-Bromo-2′-deoxyuridine
BSA	Bovine serum albumin
C57BL/6	Wild-type mouse stain
CA1, CA3	Corneu ammons 1 and 3 of the hippocampus
CD68	Cluster of differentiation 68, lysosomal phagocytotic marker
cFos	Neuronal plasticity-related immediate early gene
Con	Control
CRCI	Cancer-related cognitive impairments
DCX	Doublecortin
DG	Dentate gyrus
ELISA	Enzyme-linked immunosorbent assay
EPM	Elevated plus maze
FDA	Food and Drug Administration
FE	Fear extinction memory test
GCL	Granule cell layer of the hippocampus
Gy	Gray, unit of absorbed radiation dose
HD	Huntington's disease
Hz	Hertz
IACUC	Institutional Animal Care and Use Committee
IBA1	Ionized calcium binding adapter 1
IEG	Immediate early gene
IP	Intra-peritoneal injection
LTP	Long-term potentiation
mA	Milli ampere
MERFISH	Multiplexed error-robust fluorescence in situ hybridization
MERSCOPE	MERFISH imaging and analytical platform
MI	Memory index
mRNA	Messenger ribonucleic acid
MS	Multiple sclerosis
NA	Numerical aperture
NeuN	Neuronal nuclear antigen
NIH	The US National Institutes of Health
NPC	Neural percussor cell
NPER	Neuronal protein extraction reagent
Nptx1	Neuronal pentraxin 1
OFT	Open field test
OLM	Object location memory
PBS	Phosphate-buffered saline
pCREB	Phosphorylated cAMP-response element binding protein
PFA	Paraformaldehyde
PMSF	Phenyl-methylsulfonyl fluoride
RICD	Radiation-induced cognitive dysfunction
RO	Reverse osmosis
RT	Radiation therapy
RZ	Riluzole
SEM	Standard error of mean
SGZ	Sub-granular zone of the hippocampus
SmART	Small animal radiation therapy equipment
TTX	Triton X-100
UCI	University of California at Irvine
Veh	Vehicle

Supplementary Information

The online version contains supplementary material available at https://doi.org/10.1186/s40478-024-01906-9.

Supplementary Material 1.

Author contributions

Conception and design: AC, MMADevelopment of methodology: SMK, ARV, ACDL, ZT, XXAcquisition of data: SMK, ARV, ACDL, ZT, MDAnalysis and interpretation of data: SMK, DQN, JEB, ZT, MD, KGJ, XX, AC, MMAWriting, review and/or revision of the manuscript: SMK, ARV, DQN, JEB, ZT, XX, AC, MMAAdministrative, technical, or material support: JEB, XX, AC, MMA.Study supervision: JEB, XX, AC, MMA.Funding sources: NIH funded this research as enlisted in the paper. The content is solely the responsibility of the authors and does not necessarily represent the official views of the NIH.

Funding

This work was supported by the National Institutes of Health (NIH) awards R01CA262213 (MMA) and R01CA276212 (MMA, AC), University of California Irvine (UCI) Institute of Clinical and Translational Sciences (ICTS) Pilot award through the NIH National Center for Advancing Translational Sciences (NCATS) award UL1TR001414 (MMA, AC). We also thank the support of the UCI CFCCC Biostatistics shared resource supported by the National Cancer Institute (NIH, award P30CA062203), and UCI Center for Neural Circuit and Mapping (CNCM). The content is solely the responsibility of the authors and does not necessarily represent the official views of the NIH.

Availability of data and materials

All data and materials are available per a reasonable request. The transcriptomics data is accessible via the Gene Expression Omnibus.

Declarations

Ethics approval and consent to participate

All animal experiments were approved by the UCI Institutional Animal Care and Use Committee (IACUC)

Consent to participate

Not applicable

Consent for publication

Not applicable

Competing interests

The authors declare no competing interests.

Author details

[1]Department of Anatomy and Neurobiology, School of Medicine, University of California, Irvine, USA. [2]Department of Radiation Oncology, School of Medicine, University of California, Irvine, USA. [3]Center for Neural Circuit Mapping, School of Medicine, University of California, Irvine, USA. [4]Department of Clinical Pharmacy Practice, School of Pharmacy and Pharmaceutical Sciences, University of California, Irvine, USA. [5]Department of Pharmaceutical Sciences, School of Pharmacy and Pharmaceutical Sciences, University of California, Irvine, USA.

Received: 1 September 2024 Accepted: 29 November 2024
Published online: 18 December 2024

References

1. Acharya MM, Baulch JE, Lusardi T, Allen BD, Chmielewski NN, Baddour AAD, Limoli CL, Boison D (2016) Adenosine Kinase inhibition protects against cranial radiation-induced cognitive dysfunction. Front Mol Neurosci 9:1–10. https://doi.org/10.3389/fnmol.2016.00042
2. Acharya MM, Christie LA, Lan ML, Giedzinski E, Fike JR, Rosi S, Limoli CL (2011) Human neural stem cell transplantation ameliorates radiation-induced cognitive dysfunction. Cancer Res 71:4834–4845. https://doi.org/10.1158/0008-5472.CAN-11-0027
3. Acharya MM, Christie LA, Lan ML, Limoli CL (2013) Comparing the functional consequences of human stem cell transplantation in the irradiated rat brain. Cell Transplant 22:55–64. https://doi.org/10.3727/096368912X640565
4. Acharya MM, Green KN, Allen BD, Najafi AR, Syage A, Minasyan H, Le MT, Kawashita T, Giedzinski E, Parihar VK et al (2016) Elimination of microglia improves cognitive function following cranial irradiation. Sci Rep 6:31545. https://doi.org/10.1038/srep31545
5. Acharya MM, Martirosian V, Chmielewski NN, Hanna N, Tran KK, Liao AC, Christie LA, Parihar VK, Limoli CL (2015) Stem cell transplantation reverses chemotherapy-induced cognitive dysfunction. Cancer Res 75:676–686. https://doi.org/10.1158/0008-5472.CAN-14-2237
6. Acharya MM, Patel NH, Craver BM, Tran KK, Giedzinski E, Tseng BP, Parihar VK, Limoli CL (2015) Consequences of low dose ionizing radiation exposure on the hippocampal microenvironment. PLoS ONE 10:e0128316. https://doi.org/10.1371/journal.pone.0128316
7. Alaghband Y, Allen BD, Kramar EA, Zhang R, Drayson OGG, Ru N, Petit B, Almeida A, Doan NL, Wood MA et al (2023) Uncovering the protective neurologic mechanisms of hypofractionated FLASH radiotherapy. Cancer Res Commun 3:725–737. https://doi.org/10.1158/2767-9764.CRC-23-0117
8. Allen BD, Acharya MM, Lu C, Giedzinski E, Chmielewski NN, Quach D, Hefferan M, Johe KK, Limoli CL (2018) Remediation of radiation-induced cognitive dysfunction through oral administration of the neuroprotective compound NSI-189. Radiat Res 189:345–353. https://doi.org/10.1667/RR14879.1
9. Allen BD, Apodaca LA, Syage AR, Markarian M, Baddour AAD, Minasyan H, Alikhani L, Lu C, West BL, Giedzinski E et al (2019) Attenuation of neuroinflammation reverses adriamycin-induced cognitive impairments. Acta Neuropathol Commun 7:186. https://doi.org/10.1186/s40478-019-0838-8
10. Barres BA, Raff MC (1999) Axonal control of oligodendrocyte development. J Cell Biol 147:1123–1128. https://doi.org/10.1083/jcb.147.6.1123
11. Bathina S, Das UN (2015) Brain-derived neurotrophic factor and its clinical implications. Arch Med Sci 11:1164–1178. https://doi.org/10.5114/aoms.2015.56342
12. Benjamini Y, Hochberg Y (1995) Controlling the false discovery rate: a practical and powerful approach to multiple testing. J R Stat Soc Ser B (Methodol) 57:289–300. https://doi.org/10.1111/j.2517-6161.1995.tb02031.x
13. Calabrese F, Rossetti AC, Racagni G, Gass P, Riva MA, Molteni R (2014) Brain-derived neurotrophic factor: a bridge between inflammation and neuroplasticity. Front Cell Neurosci 8:430. https://doi.org/10.3389/fncel.2014.00430
14. Christie LA, Acharya MM, Parihar VK, Nguyen A, Martirosian V, Limoli CL (2012) Impaired cognitive function and hippocampal neurogenesis following cancer chemotherapy. Clin Cancer Res Off J Am Assoc Cancer Res 18:1954–1965. https://doi.org/10.1158/1078-0432.CCR-11-2000
15. Gomez-Pineda VG, Torres-Cruz FM, Vivar-Cortes CI, Hernandez-Echeagaray E (2018) Neurotrophin-3 restores synaptic plasticity in the striatum of a mouse model of Huntington's disease. CNS Neurosci Ther 24:353–363. https://doi.org/10.1111/cns.12824
16. de San G, Jose N, Massa F, Halbgebauer S, Oeckl P, Steinacker P, Otto M (2022) Neuronal pentraxins as biomarkers of synaptic activity: from physiological functions to pathological changes in neurodegeneration. J Neural Transm (Vienna) 129:207–230. https://doi.org/10.1007/s00702-021-02411-2
17. Greene-Schloesser D, Moore E, Robbins ME (2013) Molecular pathways: radiation-induced cognitive impairment. Clin Cancer Res Off J Am Assoc Cancer Res 19:2294–2300. https://doi.org/10.1158/1078-0432.CCR-11-2903
18. Hascup KN, Findley CA, Britz J, Esperant-Hilaire N, Broderick SO, Delfino K, Tischkau S, Bartke A, Hascup ER (2021) Riluzole attenuates glutamatergic tone and cognitive decline in AbetaPP/PS1 mice. J Neurochem 156:513–523. https://doi.org/10.1111/jnc.15224
19. Hinkle JJ, Olschowka JA, Love TM, Williams JP, O'Banion MK (2019) Cranial irradiation mediated spine loss is sex-specific and complement receptor-3 dependent in male mice. Sci Rep 9:18899. https://doi.org/10.1038/s41598-019-55366-6
20. Hinkle JJ, Olschowka JA, Williams JP, O'Banion MK (2023) Pharmacologic manipulation of complement receptor 3 prevents dendritic spine loss and cognitive impairment after acute cranial radiation. Int J Radiat Oncol Biol Phys. https://doi.org/10.1016/j.ijrobp.2023.12.017
21. Hunsberger HC, Weitzner DS, Rudy CC, Hickman JE, Libell EM, Speer RR, Gerhardt GA, Reed MN (2015) Riluzole rescues glutamate alterations, cognitive deficits, and tau pathology associated with P301L tau expression. J Neurochem 135:381–394. https://doi.org/10.1111/jnc.13230
22. Ifejeokwu OV, Do A, El Khatib SM, Ho NH, Zavala A, Othy S, Acharya MM (2024) Immune Checkpoint Inhibition-related Neuroinflammation Disrupts Cognitive Function. bioRxiv. https://doi.org/10.1101/2024.07.01.601087
23. Jehn CF, Becker B, Flath B, Nogai H, Vuong L, Schmid P, Luftner D (2015) Neurocognitive function, brain-derived neurotrophic factor (BDNF) and IL-6 levels in cancer patients with depression. J Neuroimmunol 287:88–92. https://doi.org/10.1016/j.jneuroim.2015.08.012
24. Ji JF, Ji SJ, Sun R, Li K, Zhang Y, Zhang LY, Tian Y (2014) Forced running exercise attenuates hippocampal neurogenesis impairment and the neurocognitive deficits induced by whole-brain irradiation via the BDNF-mediated pathway. Biochem Biophys Res Commun 443:646–651. https://doi.org/10.1016/j.bbrc.2013.12.031
25. Ji S, Tian Y, Lu Y, Sun R, Ji J, Zhang L, Duan S (2014) Irradiation-induced hippocampal neurogenesis impairment is associated with epigenetic regulation of bdnf gene transcription. Brain Res 1577:77–88. https://doi.org/10.1016/j.brainres.2014.06.035
26. Johnson DR, Sawyer AM, Meyers CA, O'Neill BP, Wefel JS (2012) Early measures of cognitive function predict survival in patients with newly diagnosed glioblastoma. Neuro Oncol 14:808–816. https://doi.org/10.1093/neuonc/nos082
27. Johnston KG, Berackey BT, Tran KM, Gelber A, Yu Z, MacGregor GR, Mukamel EA, Tan Z, Green KN, Xu X (2024) Single-cell spatial transcriptomics reveals distinct patterns of dysregulation in non-neuronal and neuronal cells induced by the Trem 2(R47H) Alzheimer's risk gene mutation. Mol Psychiatry. https://doi.org/10.1038/s41380-024-02651-0
28. Kang H, Sun LD, Atkins CM, Soderling TR, Wilson MA, Tonegawa S (2001) An important role of neural activity-dependent CaMKIV signaling in the consolidation of long-term memory. Cell 106:771–783. https://doi.org/10.1016/s0092-8674(01)00497-4
29. Krattli RP, Do AH, El-Khatib SM, Alikhani L, Markarian M, Vagadia AR, Usmani MT, Madan S, Baulch JE, Clark RJ et al (2024) Complement C5a receptor 1 blockade reverses cognitive deficits following cranial radiation therapy for brain cancer. bioRxiv. https://doi.org/10.1101/2024.07.02.601806
30. Leal G, Bramham CR, Duarte CB (2017) BDNF and hippocampal synaptic plasticity. Vitam Horm 104:153–195. https://doi.org/10.1016/bs.vh.2016.10.004
31. Lee KH, Lee H, Yang CH, Ko JS, Park CH, Woo RS, Kim JY, Sun W, Kim JH, Ho WK et al (2015) Bidirectional signaling of neuregulin-2 mediates formation of GABAergic synapses and maturation of glutamatergic synapses in newborn granule cells of postnatal hippocampus. J Neurosci 35:16479–16493. https://doi.org/10.1523/JNEUROSCI.1585-15.2015
32. Lesuis SL, Kaplick PM, Lucassen PJ, Krugers HJ (2019) Treatment with the glutamate modulator riluzole prevents early life stress-induced cognitive deficits and impairments in synaptic plasticity in APPswe/PS1dE9 mice. Neuropharmacology 150:175–183. https://doi.org/10.1016/j.neuropharm.2019.02.023
33. Liao AC, Craver BM, Tseng BP, Tran KK, Parihar VK, Acharya MM, Limoli CL (2013) Mitochondrial-targeted human catalase affords neuroprotection from proton irradiation. Radiat Res 180:1–6. https://doi.org/10.1667/RR3339.1
34. Lima Giacobbo B, Doorduin J, Klein HC, Dierckx R, Bromberg E, de Vries EFJ (2019) Brain-derived neurotrophic factor in brain disorders: focus on neuroinflammation. Mol Neurobiol 56:3295–3312. https://doi.org/10.1007/s12035-018-1283-6

35. Limoli CL, Kramar EA, Almeida A, Petit B, Grilj V, Baulch JE, Ballesteros-Zebadua P, Loo BW Jr, Wood MA, Vozenin MC (2023) The sparing effect of FLASH-RT on synaptic plasticity is maintained in mice with standard fractionation. Radiother Oncol 186:109767. https://doi.org/10.1016/j.radonc.2023.109767
36. Lin YJ, Hsin IL, Sun HS, Lin S, Lai YL, Chen HY, Chen TY, Chen YP, Shen YT, Wu HM (2018) NTF3 is a novel target gene of the transcription factor POU3F2 and is required for neuronal differentiation. Mol Neurobiol 55:8403–8413. https://doi.org/10.1007/s12035-018-0995-y
37. Longart M, Calderón C, González M, Grela ME, Martínez JC (2022) Neuregulins: subcellular localization, signaling pathways and their relationship with neuroplasticity and neurological diseases. Explor Neurosci 1:31–53. https://doi.org/10.37349/en.2022.00003
38. Lu B, Nagappan G, Lu Y (2014) BDNF and synaptic plasticity, cognitive function, and dysfunction. Handb Exp Pharmacol 220:223–250. https://doi.org/10.1007/978-3-642-45106-5_9
39. Makale MT, McDonald CR, Hattangadi-Gluth JA, Kesari S (2017) Mechanisms of radiotherapy-associated cognitive disability in patients with brain tumours. Nat Rev Neurol 13:52–64. https://doi.org/10.1038/nrneurol.2016.185
40. Markarian M, Krattli RP Jr, Baddour JD, Alikhani L, Giedzinski E, Usmani MT, Agrawal A, Baulch JE, Tenner AJ, Acharya MM (2021) Glia-selective deletion of complement C1q prevents radiation-induced cognitive deficits and neuroinflammation. Cancer Res 81:1732–1744. https://doi.org/10.1158/0008-5472.CAN-20-2565
41. Mizuta I, Ohta M, Ohta K, Nishimura M, Mizuta E, Kuno S (2001) Riluzole stimulates nerve growth factor, brain-derived neurotrophic factor and glial cell line-derived neurotrophic factor synthesis in cultured mouse astrocytes. Neurosci Lett 310:117–120. https://doi.org/10.1016/s0304-3940(01)02098-5
42. Montay-Gruel P, Acharya MM, Petersson K, Alikhani L, Yakkala C, Allen BD, Ollivier J, Petit B, Jorge PG, Syage AR et al (2019) Long-term neurocognitive benefits of FLASH radiotherapy driven by reduced reactive oxygen species. Proc Natl Acad Sci USA 116:10943–10951. https://doi.org/10.1073/pnas.1901777116
43. Ng DQ, Chan D, Acharya MM, Grill JD, Chan A (2023) Research attitude and interest among cancer survivors with or without cognitive impairment. Cancers (Basel). https://doi.org/10.3390/cancers15133409
44. Ng DQ, Chan D, Agrawal P, Zhao W, Xu X, Acharya M, Chan A (2022) Evidence of brain-derived neurotrophic factor in ameliorating cancer-related cognitive impairment: a systematic review of human studies. Crit Rev Oncol Hematol 176:103748. https://doi.org/10.1016/j.critrevonc.2022.103748
45. Ng DQ, Cheng I, Wang C, Tan CJ, Toh YL, Koh YQ, Ke Y, Foo KM, Chan RJ, Ho HK et al (2023) Brain-derived neurotrophic factor as a biomarker in cancer-related cognitive impairment among adolescent and young adult cancer patients. Sci Rep 13:16298. https://doi.org/10.1038/s41598-023-43581-1
46. Parihar VK, Acharya MM, Roa DE, Bosch O, Christie LA, Limoli CL (2014) Defining functional changes in the brain caused by trageted stereotaxic radiosurgery. Transl Cancer Res 3:124–137. https://doi.org/10.3978/j.issn.2218-676X.2013.06.02
47. Qin T, Guo L, Wang X, Zhou G, Liu L, Zhang Z, Ding G (2024) Repetitive transcranial magnetic stimulation ameliorates cognitive deficits in mice with radiation-induced brain injury by attenuating microglial pyroptosis and promoting neurogenesis via BDNF pathway. Cell Commun Signal 22:216. https://doi.org/10.1186/s12964-024-01591-0
48. Sakamoto K, Karelina K, Obrietan K (2011) CREB: a multifaceted regulator of neuronal plasticity and protection. J Neurochem 116:1–9. https://doi.org/10.1111/j.1471-4159.2010.07080.x
49. Shimazu K, Zhao M, Sakata K, Akbarian S, Bates B, Jaenisch R, Lu B (2006) NT-3 facilitates hippocampal plasticity and learning and memory by regulating neurogenesis. Learn Mem 13:307–315. https://doi.org/10.1101/lm.76006
50. Usmani MT, Krattli RP Jr, El-Khatib SM, Le ACD, Smith SM, Baulch JE, Ng DQ, Acharya MM, Chan A (2023) BDNF augmentation using riluzole reverses doxorubicin-induced decline in cognitive function and neurogenesis. Neurotherapeutics 20:838–852. https://doi.org/10.1007/s13311-022-01339-z
51. Voss MW, Vivar C, Kramer AF, van Praag H (2013) Bridging animal and human models of exercise-induced brain plasticity. Trends Cogn Sci 17:525–544. https://doi.org/10.1016/j.tics.2013.08.001
52. Welzel G, Fleckenstein K, Schaefer J, Hermann B, Kraus-Tiefenbacher U, Mai SK, Wenz F (2008) Memory function before and after whole brain radiotherapy in patients with and without brain metastases. Int J Radiat Oncol Biol Phys 72:1311–1318. https://doi.org/10.1016/j.ijrobp.2008.03.009
53. Wilcoxon F (1992) Individual comparisons by ranking methods. In: Kotz S, Johnson NL (eds) Breakthroughs in statistics: methodology and distribution. Springer, New York, City, pp 196–202
54. Winocur G, Wojtowicz JM, Huang J, Tannock IF (2014) Physical exercise prevents suppression of hippocampal neurogenesis and reduces cognitive impairment in chemotherapy-treated rats. Psychopharmacology 231:2311–2320. https://doi.org/10.1007/s00213-013-3394-0
55. Wymer J, Apple S, Harrison A, Hill BA (2023) Pharmacokinetics, bioavailability, and swallowing safety with riluzole oral film. Clin Pharmacol Drug Dev 12:57–64. https://doi.org/10.1002/cpdd.1168
56. Yucel B, Akkas EA, Okur Y, Eren AA, Eren MF, Karapinar H, Babacan NA, Kilickap S (2014) The impact of radiotherapy on quality of life for cancer patients: a longitudinal study. Support Care Cancer Off J Multinational Assoc Support Care Cancer 22:2479–2487. https://doi.org/10.1007/s00520-014-2235-y
57. Zeng H, Huang J, Ren J, Wang CK, Tang Z, Zhou H, Zhou Y, Shi H, Aditham A, Sui X et al (2023) Spatially resolved single-cell translatomics at molecular resolution. Science 380:eadd3067. https://doi.org/10.1126/science.add3067
58. Zhang M, Pan X, Jung W, Halpern AR, Eichhorn SW, Lei Z, Cohen L, Smith KA, Tasic B, Yao Z et al (2023) Molecularly defined and spatially resolved cell atlas of the whole mouse brain. Nature 624:343–354. https://doi.org/10.1038/s41586-023-06808-9

Publisher's Note